Infrared and ab Initio Studies on 1,2,4,5-Tetrafluorobenzene Clusters with Methanol and 2,2,2-Trifluoroethanol: Presence and Absence of an Aromatic C−H···O Hydrogen Bond

V. Venkatesan, A. Fujii, T. Ebata, and N. Mikami*

Department of Chemistry, Graduate School of Science, Tohoku University, Sendai 980-8578, Japan

Received: August 26, 2004

The (1:1) clusters of 1,2,4,5-tetrafluorobenzene (TFB) with methanol and with 2,2,2-trifluoroethanol (TFE) were studied both experimentally and computationally. Through use of fluorescence-detected infrared spectroscopy, the (1:1) clusters were identified in supersonic jets. Intermolecular interactions in the clusters were characterized by the spectral shifts of the aromatic C−H stretching modes in the TFB moiety owing to the cluster formation. The molecular structures, stabilization energies, and vibrational frequencies of the clusters were computed at the MP2/6-31+G* level. Both computational and experimental data indicate that an aromatic C−H···O hydrogen bond is present in the TFB−methanol cluster, while it is absent in the TFB−TFE cluster.

Introduction

Hydrogen bonds have attracted substantial interest in the fields of chemistry and biology.[1,2] Depending on the type of the interaction, the strength of the hydrogen bond can vary from well over 10 kcal/mol (termed as strong hydrogen bonds) to a few kcal/mol (weak hydrogen bonds). Though the stabilization energy of the weak hydrogen bond is generally quite small, it has been pointed out that such a weak intermolecular interaction is of potential importance in structures and functions of biological macromolecules. Therefore, a great deal of effort has been made to understand the nature of weak hydrogen bonds. The C−H···O hydrogen bond is one of the weakest hydrogen bonds, and a number of studies have been carried out as seen in the literature.[2−5] In particular, aromatic C−H···O hydrogen bonds are of considerable interest in crystal engineering, biological systems, and molecular recognition.[6−14] For the investigation of such a weak aromatic C−H···O hydrogen bond, vibrational spectroscopy is one of the most powerful techniques. Moreover, combination with supersonic jet spectroscopy is ideally suited for such studies because it allows us to observe intermolecular interactions without perturbations from surrounding molecules. Recently, Kim, Brutschy, and co-workers[15−19] indicated the formation of an aromatic C−H···O hydrogen bond in mono- and disubstituted halobenzene−water/methanol clusters by infrared depletion spectroscopy combined with ab initio calculations. Since the aromatic C−H stretch region in infrared spectra is usually congested due to several bands including Fermi resonance counterparts, it is not so straightforward to extract the structural information from the spectra. More recently, we reported an experimental and computational study on the 1,2,4,5-tetrafluorobenzene (TFB)−water cluster.[20] It showed a clear low-frequency shift and intensity enhancement of the aromatic C−H stretching vibration of the TFB moiety upon cluster formation. This was the first direct experimental evidence for an aromatic C−H···O hydrogen bond in isolated gas-phase clusters. In addition to the aromatic C−H···O interaction, the computational data indicated the presence of another interaction (i.e., O−H···F interaction) to stabilize the TFB−water cluster. The combination of these interactions prefers to have an in-plane (ring) type structure in the TFB−water cluster. If any one of the interactions is absent or significantly enhanced, then it would result in a different cluster structure, demonstrating the competition between the aromatic C−H···O hydrogen bond and the other intermolecular interactions.

With respect to this point, in this study, we have tried to compare the TFB−methanol and TFB−2,2,2-trifluoroethanol (TFE) systems. The presence of the electron-withdrawing CF_3 group in TFE enhances the acidity of the hydroxyl group, and it may change the balance between the intermolecular interactions. We apply both electronic and vibrational spectroscopy to identify and characterize the 1:1 clusters of TFB−methanol and TFB−TFE in the isolated gas-phase condition. We also perform ab initio computations on the structures, energies, and vibrational frequencies of the TFB−methanol and TFB−TFE clusters at the MP2/6-31+G* level to corroborate our experimental results.

Experimental Section

The details of the experimental setup have been described elsewhere.[21] Briefly, laser-induced fluorescence (LIF) excitation, fluorescence-detected infrared (FDIR), and infrared−ultraviolet (IR−UV) hole-burning spectra were recorded on a jet expansion of TFB with methanol or TFE. TFB (Aldrich, >99%), methanol (Cica, >99%), and TFE (Cica, >98%) were used without further purification. The gaseous mixture of TFB and methanol (or TFE) was seeded in a helium buffer gas of stagnation pressure at 2−4 atm and was expanded by a pulsed nozzle with an orifice of 0.8 mm diameter. The LIF signal was detected by a photomultiplier tube (Hamamatsu, 1P28) combined with color filters. The IR spectrum of the cluster was obtained by FDIR spectroscopy. In this spectroscopy, the ground-state population of a particular species is monitored as the LIF intensity of the $S_1 \leftarrow S_0$ transition with a UV laser pulse. A tunable IR laser pulse is introduced 50 ns prior to the UV pulse. When the IR frequency is resonant with the vibrational transition of the species monitored, the ground-state population decreases, resulting in the depletion of the LIF signal intensity. Thus, the IR spectrum is obtained as a fluorescence dip spectrum. To identify the existence of multiple isomers, we employed IR−UV hole-

* Corresponding author. Fax: +81-22-217-6785. E-mail: nmikami@qclhp.chem.tohoku.ac.jp.

10.1021/jp046153g CCC: $30.25
Published on Web 01/12/2005

burning spectroscopy. In this technique, the LIF excitation spectra with the UV laser pulse are recorded with and without the IR pulse tuned to a vibrational transition of a particular isomer, where the IR pulse is introduced at 50 ns prior to the UV pulse. In comparison with the band intensities in these two spectra, only the bands due to the isomer labeled by the vibrational transition show the intensity decrease with the IR light.

Computational Methods

Ab initio computations on the TFB−methanol and TFB−TFE systems were performed using the Gaussian 98 program.[22] Geometry optimizations were performed at the MP2/6-31+G* level to obtain minima corresponding to the various isomers of the TFB−methanol and TFB−TFE clusters. The choice of this level has already been proven to be applicable to a larger number of clusters containing π systems.[23] No constraints were imposed on the molecular geometry during the optimization process. The stabilization energies of the clusters were corrected for the zero-point energy (ZPE) and basis set superposition error (BSSE) using the counterpoise correction scheme outlined by Boys and Bernardi.[24] According to Kim et al.,[23] the 100% BSSE correction often underestimates the stabilization energy, and the 50% correction is a good empirical approximation. Therefore, we report the stabilization energies with both the 100% and 50% BSSE corrections. Vibrational frequencies of each isomer were also calculated at the MP2/6-31+G* level. The computed frequencies were then scaled to fit to the experimental results. The scaling factor of 0.9482 was determined to reproduce the observed aromatic C−H stretching frequency of bare TFB.

The computed frequencies of the isomers of the TFB−methanol and TFB−TFE clusters were then used to simulate the vibrational spectra. Simulated spectra were constructed assuming a Lorentzian line profile with a full-width half-maximum (fwhm) of 0.5 cm^{-1}, which is the typical line width obtained in our experimental spectra.

Results and Discussion

Experimental. The identification of the electronic transition corresponding to the binary cluster is the first step in the spectroscopic characterization. Figure 1a shows the $S_1 \leftarrow S_0$ LIF excitation spectrum of TFB in the region of 36 500−37 160 cm^{-1}. A strong band at 36 555 cm^{-1} is assigned to the origin band of TFB as reported in the literature.[25] When TFB is coexpanded with methanol, new features at 36 776, 36 806, 36 832, 36 845, and 36 846 cm^{-1} appeared in the spectrum (Figure 1b). These features are clearly attributed to the clusters of TFB with methanol. The features of TFB−methanol are high-frequency-shifted by 221, 251, 277, 290, and 291 cm^{-1} from the origin band of bare TFB. Figure 1c shows the LIF excitation spectrum of TFB in the presence of TFE. In this case, new features appear at the high-frequency side by 111, 125, 128, 175, 185, and 188 cm^{-1} from the origin band of bare TFB. These observations are quite similar with the case of TFB−water in which the cluster bands are high-frequency-shifted by 198 and 255 cm^{-1}.[20] Through use of IR−UV hole-burning spectroscopy, we confirmed that all of the cluster features of TFB−methanol and TFB−TFE are due to a single isomer of the (1:1) cluster, as will be discussed later. We also note that the features seen at 36 753 and 36 810 cm^{-1} in Figure 1 are attributed to the TFB−water cluster. As water is an unavoidable impurity in such experiments, these cluster bands are seen in every spectrum.

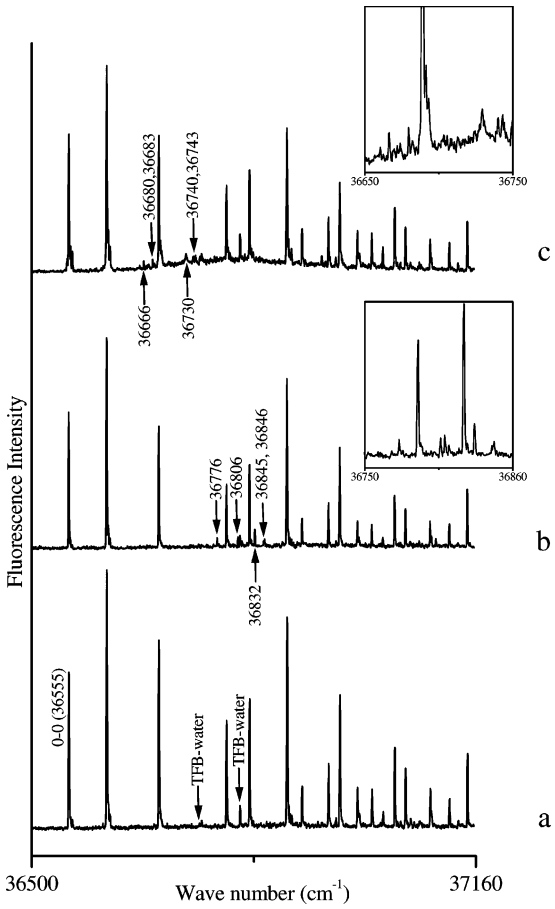

Figure 1. Laser-induced fluorescence spectra of (a) 1,2,4,5-tetrfluorobenzene (TFB), (b) TFB in the presence of methanol, and (c) TFB in the presence of 2,2,2-trifluoroethanol (TFE). Insert figures show the expanded scale for the corresponding cluster region.

The FDIR spectra of bare TFB, TFB−methanol, and TFB−TFE in the C−H and O−H stretch regions are depicted in parts b, c, and d of Figure 2, respectively. As reported in our previous study, the antisymmetric aromatic C−H stretching vibration of bare TFB shows a weak doublet at 3091 and 3094 cm^{-1} (Figure 2b), which may be attributed to a Fermi mixing.[20] In the spectrum of the TFB−methanol cluster, two bands are seen at 3082 and 3066 cm^{-1} in the aromatic C−H stretch region. A feature at 3082 cm^{-1} is assigned to the aromatic C−H stretch of the TFB moiety in the cluster. Another feature at 3066 cm^{-1} may be a combination band due to a Fermi mixing with the C−H stretch, which was also observed in the TFB−water cluster.[20] The aromatic C−H stretch frequency of TFB−methanol is low-frequency-shifted by 12 cm^{-1} in comparison with that of 3094 cm^{-1} in bare TFB. This low-frequency shift clearly indicates the formation of an aromatic C−H···O hydrogen bond between the TFB and methanol molecules. It can also be seen from parts b and c of Figures 2 that the intensity of the aromatic C−H band in the TFB−methanol cluster is significantly enhanced in comparison with that of bare TFB. It further supports the formation of the aromatic C−H···O hydrogen bond, which substantially perturbs the aromatic C−H stretch of the TFB moiety in the cluster. The O−H stretching band of the methanol moiety in the TFB−methanol cluster is observed at 3668 cm^{-1} (Figure 2c). The O−H stretch mode is low-frequency-shifted by 13 cm^{-1} from that of bare methanol.[26] The C−H stretching frequencies of the methanol moiety in the TFB−methanol cluster are observed at 3004, 2959, and 2848 cm^{-1}, which are close to those of the υ_2 (2999 cm^{-1}), υ_9 (2959

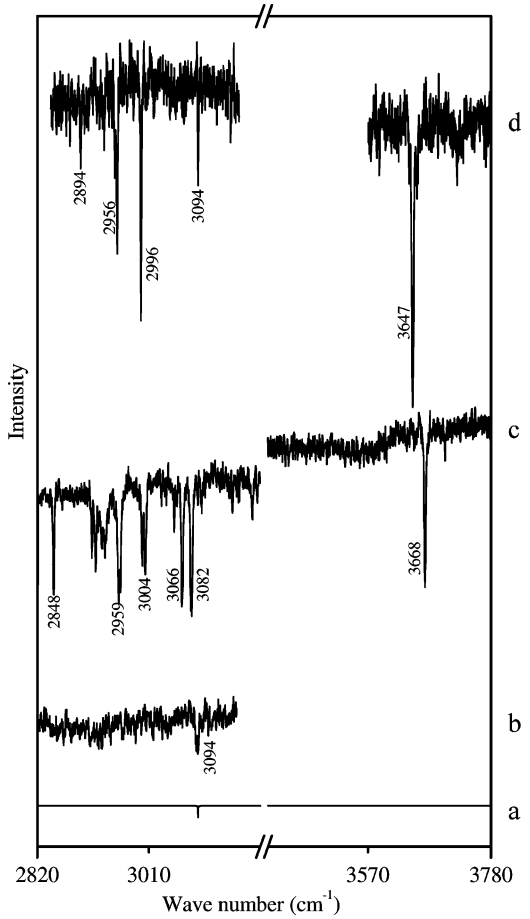

Figure 2. Experimental and computed infrared spectra in the C−H and O−H stretching vibrational regions. (a) Computed spectrum for bare TFB. Fluorescence-detected infrared spectra of (b) bare TFB, (c) TFB−methanol, and (d) TFB−TFE.

cm^{-1}), and υ_3 (2843 cm^{-1}) modes of bare methanol, respectively.[27,28] We also observed the overtone and combination bands of the bending vibrations of the methanol moiety near 2915 cm^{-1}. The similar bands were also observed in the studies on the fluorobenzene−methanol and *p*-difluorobenzene−methanol clusters.[17] The observed vibrational frequencies of the TFB−methanol cluster are tabulated in Table 1.

In contrast with TFB−methanol, the aromatic C−H stretching band of the TFB moiety in TFB−TFE is observed at 3094 cm^{-1} (Figure 2d), which is same as that of bare TFB. Moreover, no remarkable enhancement of the band intensity was seen. These characteristics clearly indicate that the aromatic C−H···O hydrogen bond is absent in TFB−TFE. The O−H stretching band of the TFE moiety is observed at 3647 cm^{-1}. The O−H stretch mode is low-frequency-shifted by 10 cm^{-1} from that of bare TFE.[29] The C−H frequencies of the TFE moiety are observed at 2996, 2956, and 2894 cm^{-1}, which are close to those of the CH_2 antisymmetric stretch ($\upsilon_2 = 2992$ cm^{-1}), CH_2 symmetric stretch ($\upsilon_3 = 2949$ cm^{-1}), and overtone of CH_2 deformation ($2\upsilon_4 = 2896$ cm^{-1}) modes of bare TFE, respectively.[29] The observed vibrational frequencies of TFB−TFE are tabulated in Table 2.

The existence of multiple isomers, even in the binary clusters, is known in many instances. To investigate such a possibility, IR−UV hole-burning spectroscopy was applied to the TFB−methanol and TFB−TFE systems. The IR−UV hole-burning spectra for TFB−methanol and TFB−TFE are shown in Figures 1S and 2S in the Supporting Information. All of the cluster bands of the TFB−methanol cluster show a decrease in intensity with the introduction of the IR light of which the wavelength is resonant with the O−H stretching vibration. The same is observed also for TFB−TFE. It confirms that all of the corresponding cluster bands of TFB−methanol and TFB−TFE arise from a single isomer of their (1:1) cluster.

From the above experimental results, it is evident that the TFB−methanol cluster has a structure involving an aromatic C−H···O hydrogen bond, while such a bond is absent in TFB−TFE.

Computational. At the outset, we performed geometry optimizations at the MP2 level using a 6-31+G* basis set. In the case of TFB−methanol, we have found three minima corresponding to the **1A**, **1B**, and **1C** structures as shown in Figure 3. Interestingly, the **1B** type isomer does not show a minimum in the case of the TFB−water system. In isomer **1A**, the interatomic distance of H12−O14 was found to be 2.196 Å, which is substantially shorter than the sum of the van der Waals radii for this pair of atoms and is known to be a typical distance expected for an aromatic C−H···O hydrogen bond.[6] This result indicates the presence of an aromatic C−H···O hydrogen bond in isomer **1A**. In addition, we also note that the H13−F7 distance is 2.339 Å, which is within the sum of the van der Waals radii for this pair of atoms, indicating the contribution of the O−H···F hydrogen bond in isomer **1A**.[6] The in-plane (ring) type structure of isomer **1A** is similar to the most stable structure of TFB−water. On the other hand, the absence of the aromatic C−H···O hydrogen bond is clearly revealed in isomers **1B** and **1C** from their on-top geometric structures. The stabilization energies of these structures are given in Table 3. The stabilization energies are corrected for ZPE, for ZPE + 100% BSSE, and for ZPE + 50% BSSE as well. The ZPE corrections are scaled by 0.9482 because this factor fits the computed frequencies to the experimental values. The ZPE +

TABLE 1: Experimental and Computed Vibrational Frequencies (cm^{-1}) and Assignments for 1,2,4,5-Tetrafluorobenzene (TFB), Methanol, and TFB−Methanol Clusters

	computed[a]	experimental	mode assignment
TFB	3095(0)[b]		symmetric υ_{CH}
	3094(12)	3091, 3094	antisymmetric υ_{CH}
CH_3OH	3580(35)	3681[c]	υ_{OH}
	3060(21)	2999[d]	υ_2
	2992(50)	2959[d]	υ_9
	2923(57)	2843[d]	υ_3
TFB−CH_3OH **1A**	3095(4)		free υ_{CH} of TFB
	3069(103)	3082, 3066[e]	hydrogen-bonded υ_{CH} of TFB
	3567(54)	3668	υ_{OH} of CH_3OH
	3061(18)	3004	υ_2 of CH_3OH
	3003(40)	2959	υ_9 of CH_3OH
		2936, 2919, 2913	overtone and combination of υ_{bend} of CH_3OH
	2930(70)	2848	υ_3 of CH_3OH
TFB−CH_3OH **1B**	3095(3)		υ_{CH} of TFB
	3092(5)		υ_{CH} of TFB
	3567(35)		υ_{OH} of CH_3OH
	3056(17)		υ_2 of CH_3OH
	2993(44)		υ_9 of CH_3OH
	2922(47)		υ_3 of CH_3OH
TFB−CH_3OH **1C**	3095(3)		υ_{CH} of TFB
	3093(7)		υ_{CH} of TFB
	3571(37)		υ_{OH} of CH_3OH
	3053(19)		υ_2 of CH_3OH
	2995(44)		υ_9 of CH_3OH
	2924(54)		υ_3 of CH_3OH

[a] The calculation level is MP2/6-31+G*. A scaling factor of 0.9482 is applied. This scaling factor is determined to reproduce the observed frequency of bare TFB. [b] Values in parentheses are computed intensities in km/mol. [c] From ref 26. [d] From refs 27 and 28. [e] Fermi mixing (see text).

TABLE 2: Experimental and Computed Vibrational Frequencies (cm^{-1}) and Assignments for 1,2,4,5-Tetrafluorobenzene (TFB), 2,2,2-Trifluoroethanol (TFE), and TFB−TFE Clusters

	computed[a]	experimental	mode assignment
TFB	3095(0)[b]		symmetric υ_{CH}
	3094(12)	3091, 3094	antisymmetric υ_{CH}
TFE(g)	3555(55)	3657[c]	υ_{OH}
	3049(4)	2992[c]	υ_2, CH_2 antisymmetric stretch
	2956(19)	2949[c]	υ_3, CH_2 symmetric stretch
		2896[c]	$2\upsilon_4$ (υ_4: CH_2 deformation)
TFE(t)	3575(61)		υ_{OH}
	2999(13)		υ_2, CH_2 antisymmetric stretch
	2940(23)		υ_3, CH_2 symmetric stretch
		3094	υ_{CH} of TFB
		3647	υ_{OH} of TFE
		2996	υ_2 of TFE
		2956	υ_3 of TFE
		2894	$2\upsilon_4$ of TFE
TFB−TFE(g) **1D**	3099(6)		υ_{CH} of TFB
	3093(7)		υ_{CH} of TFB
	3541(73)		υ_{OH} of TFE
	3045(3)		υ_2 of TFE
	2956(21)		υ_3 of TFE
TFB−TFE(g) **1E**	3095(0)		υ_{CH} of TFB
	3094(15)		υ_{CH} of TFB
	3567(203)		υ_{OH} of TFE
	3043(6)		υ_2 of TFE
	2964(13)		υ_3 of TFE
TFB−TFE(g) **1F**	3096(3)		υ_{CH} of TFB
	3093(8)		υ_{CH} of TFB
	3543(66)		υ_{OH} of TFE
	3043(3)		υ_2 of TFE
	2956(21)		υ_3 of TFE
TFB−TFE(g) **1G**	3097(4)		υ_{CH} of TFB
	3094(7)		υ_{CH} of TFB
	3538(53)		υ_{OH} of TFE
	3047(2)		υ_2 of TFE
	2956(19)		υ_3 of TFE

[a] The calculation level is MP2/6-31+G*. A scaling factor of 0.9482 is applied. This scaling factor is determined to reproduce the observed frequency of bare TFB. [b] Values in parentheses are computed intensities in km/mol. [c] From ref 29.

50% BSSE corrected stabilization energies for the **1A**, **1B**, and **1C** isomers of TFB−methanol are 3.94, 3.02, and 3.00 kcal/mol, respectively, at the MP2/6-31+G* level. Isomer **1A** is the most stable among the isomers of TFB−methanol. Moreover, this isomer is quite similar to the most stable structure of the (1:1) cluster of the fluorobenzene−methanol and *p*-difluorobenzene−methanol systems.[17] However, the stabilization energy of isomer **1A** in TFB−methanol (3.94 kcal/mol) is larger than those in the *p*-difluorobenzene−methanol (3.40 kcal/mol) and fluorobenzene−methanol (3.22 kcal/mol) systems, being estimated at the same level of theory. This increase in the stabilization energy is accompanied by a decrease in the H12−O14 bond distance from fluorobenzene−methanol (2.393 Å) to *p*-difluorobenzene−methanol (2.326 Å) to TFB−methanol (2.196 Å). The presence of four electron-withdrawing fluorine atoms in TFB enhances the acidity of the aromatic C−H, and it results in the stronger aromatic C−H···O hydrogen bond. On the other hand, the H13−F7 distance is increased from fluorobenzene−methanol (2.086 Å) to *p*-difluorobenzene−methanol (2.128 Å) and TFB−methanol (2.339 Å). This behavior reflects the competition between the aromatic C−H···O and O−H···F hydrogen bonds, where the increase of the one hydrogen bond strength results in the decrease of the other. Similar observations are also seen in the cases of clusters of TFB, *p*-difluorobenzene, and fluorobenzene with water. TFB−water (3.63 kcal/mol) has a larger stabilization energy than those of *p*-difluorobenzene−water (2.80 kcal/mol) and fluorobenzene−water (2.68 kcal/mol).[15]

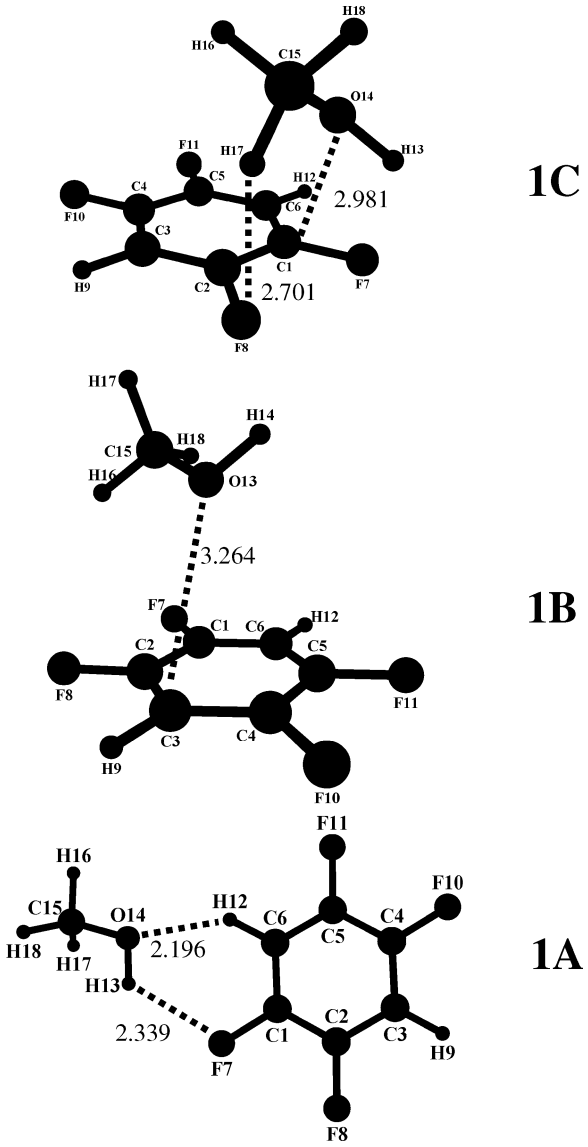

Figure 3. Structures of the TFB−methanol cluster showing selected intermolecular bond distances (Å). All calculations were performed at the MP2/6-31+G* level.

TABLE 3: Stabilization Energies (kcal/mol) for the 1,2,4,5-Tetrafluorobenzene (TFB)−Methanol and TFB−2,2,2-Trifluoroethanol (TFE) Clusters Using MP2/6-31+G* Level of Theory

		stabilization energy		
		ΔE_1[a]	ΔE_2[b]	ΔE_3[c]
TFB−CH_3OH	**1A**	4.86	3.02	3.94
	1B	4.39	1.66	3.02
	1C	4.38	1.62	3.00
TFB−TFE(g)	**1D**	6.58	2.28	4.43
	1E	5.92	2.66	4.29
	1F	6.18	1.92	4.05
	1G	5.61	2.05	3.83

[a] With ZPE correction. [b] With ZPE + 100% BSSE correction. [c] With ZPE + 50% BSSE correction.

In the geometrical optimization of TFB−TFE, using the MP2/6-31+G* level, we initially found that bare TFE has two minima corresponding to the gauche and trans forms with respect to the dihedral angle of CCOH. The gauche conformer is more stable, in agreement with the previous reports.[29−31] At the MP2/6-31+G* level, the zero-point corrected energy difference between gauche and trans conformers is 1.93 kcal/mol. We then

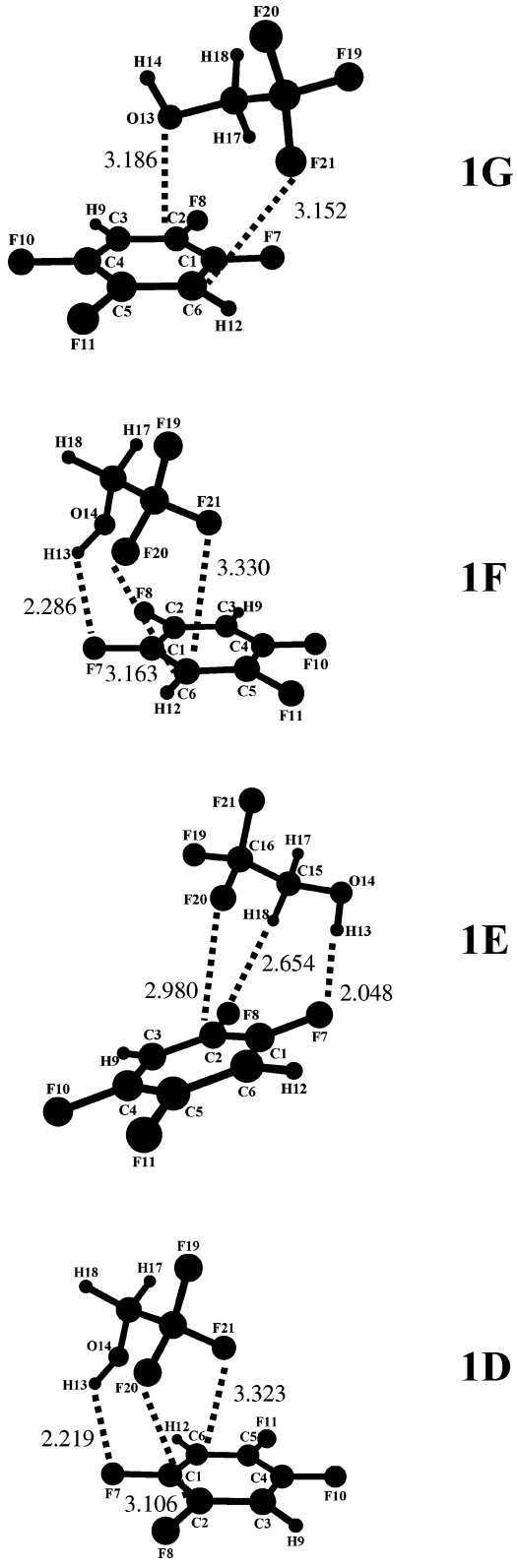

Figure 4. Structures of the TFB−TFE(g) cluster showing selected intermolecular bond distances (Å). All calculations were performed at the MP2/6-31+G* level.

examined the TFB−TFE isomers involving both of these conformers. Four minima are obtained corresponding to the TFB−TFE isomers that arise from TFB with the gauche conformer of TFE (TFE(g)): **1D**, **1E**, **1F**, and **1G** as shown in Figure 4. We also searched other possible isomers that arise from TFB with the trans conformer of TFE (TFE(t)). However, all initial geometries of the TFB−TFE(t) isomers were converged into one of the optimized TFB−TFE(g) isomers, and we did not find any optimized structure corresponding to the TFB−TFE(t) isomer. Moreover, as seen in Figure 4, all of the isomers have on-top structures, where the aromatic C−H···O hydrogen bond is clearly absent. Though we tried structures similar to the **1A** isomer of TFB−methanol, the TFE moiety was flipped on the aromatic ring surface during the optimization. The stabilization energies of the TFB−TFE(g) structures are given in Table 3. The ZPE + 50% BSSE corrected stabilization energies for **1D**, **1E**, **1F**, and **1G** isomers of TFB−TFE(g) are 4.43, 4.29, 4.05, and 3.83 kcal/mol, respectively, at the MP2/6-31+G* level. In isomers **1D**, **1E**, and **1F**, the interatomic distance of H13−F7 are 2.219, 2.048, and 2.286 Å, respectively. These distances lie within the sum of the van der Waals radii for this pair of atoms and are typical distances expected for O−H···F hydrogen bonds.[6] The interatomic distances of C2−F20 and C6−F21 in **1D** are 3.106 and 3.323 Å, respectively. The interatomic distance of C2−F20 in **1E** is 2.980 Å. The interatomic distances of C6−F20 and C6−F21 in **1F** are 3.163 and 3.330 Å, respectively. The interatomic distances of O13−C2 and C6−F21 in **1G** are 3.186 and 3.152 Å, respectively. These distances are comparable with previous results reported by Alkorta et al. for electron donor···π (C_6F_6) interactions.[32]

Vibrational Assignments. Tables 1 and 2 give the scaled computed frequencies for the isomers of TFB−methanol and TFB−TFE, respectively, optimized at the MP2/6-31+G* level together with the experimentally observed frequencies. The simulated spectra depicting the scaled frequencies are also seen in Figures 5 and 6 with the experimentally observed spectra. Figures 2a, 5b−d, and 6b−e show the computed spectra of bare TFB, TFB−methanol isomers, and TFB−TFE isomers, respectively.

As seen from Table 1 and Figure 5, the observed spectral features of TFB−methanol are well reproduced only with the simulated spectrum (Figure 5b) of isomer **1A**, which has an aromatic C−H···O hydrogen bond. The calculated results predict that the hydrogen-bonded aromatic C−H stretching gives a low-frequency shift of 25 cm^{-1} from the aromatic C−H stretch of bare TFB. Furthermore, the intensity of the hydrogen-bonded aromatic C−H stretch (103 km/mol) is significantly stronger than those in bare TFB (12 km/mol). Such a low-frequency shift and intensity enhancement of the hydrogen-bonded aromatic C−H stretch in isomer **1A** are consistent with the present experimental observation. Thus, the formation of the aromatic C−H···O hydrogen bond in TFB−methanol is clearly supported by the ab initio calculations. As in the TFB−water system, the O−H and C−H stretching frequencies of the methanol moiety of all of the isomers do not show any significant difference. It is therefore difficult to derive any structural information from these vibrations.

In contrast with the TFB−methanol cluster, the experimental results strongly suggest that the aromatic C−H···O hydrogen bond is absent in the TFB−TFE cluster. Our computations also predict that all of the stable isomers, **1D**, **1E**, **1F**, and **1G** have the on-top structures with an absence of the aromatic C−H···O hydrogen bond. As seen in Figure 6 and Table 2, the computed aromatic C−H stretch frequencies of all of these isomers very closely resemble the observed frequency. Furthermore, the computed shift values of the O−H and C−H stretching modes of the TFB moiety of all of the isomers do not agree well with the corresponding experimental values (Table 4). Hence, at present stage, we cannot identify the structure of TFB−TFE. Even though the structure determination is difficult, the absence

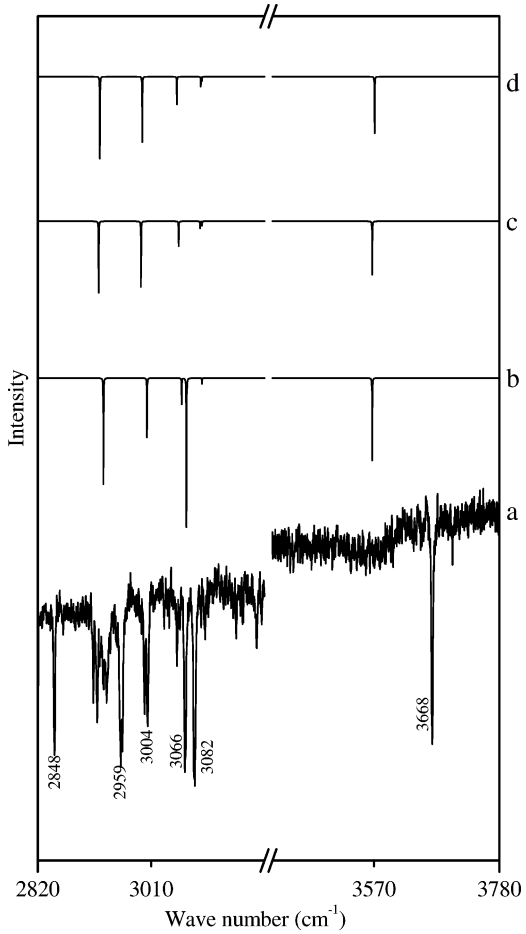

Figure 5. (a) Fluorescence-detected infrared spectra of TFB−methanol. Computed spectra of TFB−methanol in the structures of (b) **1A**, (c) **1B**, and (d) **1C** isomers. The same intensity scale was used for plotting the computed spectra.

TABLE 4: Experimental and Computed Shift Values (cm^{-1}) of O−H and C−H Stretching Vibration of 1,2,4,5-Tetrafluorobenzene (TFB)−2,2,2-Trifluoroethanol (TFE) Clusters

		computed[b]			
$\Delta\nu$[a]	experiment	**1D**	**1E**	**1F**	**1G**
$\Delta\nu_{OH}$	−10	−14	12	−12	−17
$\Delta\nu_2$	4	−4	−6	−6	−2
$\Delta\nu_3$	7	0	8	0	0

[a] $\Delta\nu = \nu_{cluster} - \nu_{bare}$. [b] Using MP2/6-31+G* level of theory.

of an aromatic C−H···O hydrogen bond in TFB−TFE is clearly supported from both the experimental and the computational results.

Comparison of TFB−Methanol, TFB−Water, and TFB−TFE Clusters. The presence and absence of an aromatic C−H···O hydrogen bond is clearly revealed in TFB−methanol and TFB−TFE clusters, respectively. The experimental and computational data indicate the enhancement of the aromatic C−H···O hydrogen bond strength in TFB−methanol in comparison with that of TFB−water. The observed shift value of the hydrogen-bonded aromatic C−H stretch in TFB−methanol (12 cm^{-1}) is larger than that in TFB−water (8 cm^{-1}). This observation is also supported by our computations, which show a shorter H12−O14 bond distance in TFB−methanol (2.196 Å) than in TFB−water (2.217 Å). The larger proton affinity of methanol (754.3 kJ/mol) than that of water (691.0 kJ/mol) reflects this difference of the aromatic C−H···O hydrogen bond strength.[33] On the other hand, in TFB−TFE, the O−H···F bond

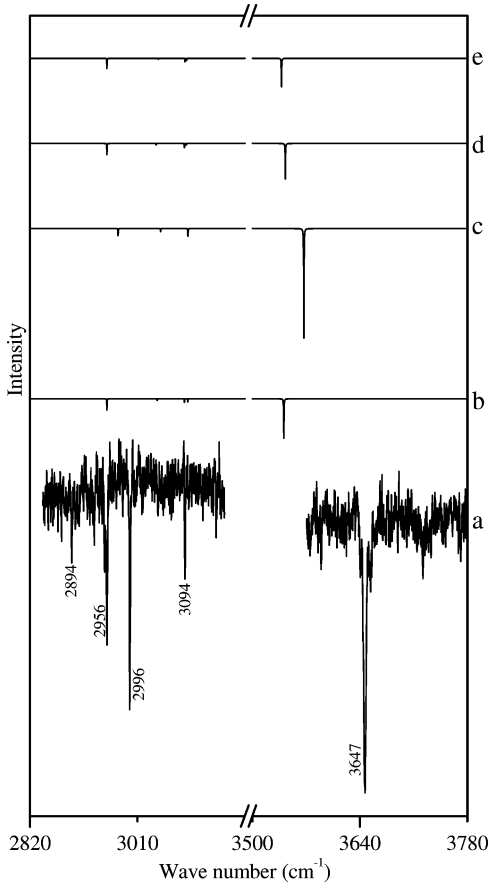

Figure 6. (a) Fluorescence-detected infrared spectra of TFB−TFE. Computed spectra of TFB−TFE(g) in the structures of (b) **1D**, (c) **1E**, (d) **1F**, and (e) **1G** isomers. The same intensity scale was used for plotting the computed spectra.

distance (2.048−2.286 Å) is shorter than that of TFB−methanol (2.339 Å), indicating the O−H···F interaction is strengthened in TFB−TFE. The larger acidity of TFE than methanol reflects this difference of the O−H···F hydrogen bond strength. Moreover, the fluorine atom(s) of the CF_3 group of TFE also show the effective interactions with the aromatic ring of TFB in all of the isomers; they might be predominant over the aromatic C−H···O hydrogen bond. This would result in the transformation of the in-plane structure to the on-top structure, which makes the absence of an aromatic C−H···O hydrogen bond in TFB−TFE.

Conclusions

Fluorescence-detected infrared spectroscopy was applied to the (1:1) clusters of TFB with methanol and 2,2,2-trifluoroethanol in a supersonic jet. The low-frequency shift and intensity enhancement of the hydrogen-bonded aromatic C−H stretching vibration clearly revealed the presence of an aromatic C−H···O hydrogen bond in TFB−methanol. On the other hand, the aromatic C−H did not show any shift in the TFB−TFE cluster, indicating the absence of an aromatic C−H···O hydrogen bond. The ab initio computations at the MP2/6-31+G* level also supported the present experimental observations.

Acknowledgment. This work has been supported by MEXT Japan, through a project (No. 16002008) of Grant-in-Aid for specifically promoted research. V.V. thanks the Center Of Excellence (COE) Foundation, Japan, for a fellowship. Part of the experimental results in this research was obtained using

supercomputing resources at the Information Synergy Center, Tohoku University, Japan.

Supporting Information Available: IR−UV hole-burning spectra for TFB−methanol and TFB−TFE clusters. This material is available free of charge via the Internet at http://pubs.acs.org.

References and Notes

(1) Pimental, G. C.; McClellan, A. L. *The Hydrogen Bond*; W. H. Freeman: San Francisco, CA, 1960.

(2) Jeffrey, G. A.; Saenger, W. *Hydrogen Bonding in Biological Structures*; Springer: Berlin, 1991.

(3) Green, R. D. *Hydrogen Bonding by C−H Groups*; Wiley-Interscience: New York, 1974.

(4) Scheiner, S. *Hydrogen Bonding: A Theoretical Perspective*; Oxford University Press: Oxford, 1997.

(5) Hobza, P.; Havlas, Z. *Chem. Rev.* **2000**, *100*, 4253.

(6) Desiraju, G. R.; Steiner, T. *The Weak Hydrogen Bond*; Oxford University Press: New York, 1999.

(7) Camilleri, P.; Eggleston, D. S.; Rzepa, H. S.; Webb, M. L. *J. Chem. Soc., Chem. Commun.* **1994**, 1135.

(8) Desiraju, G. R. *Acc. Chem. Res.* **1996**, *29*, 441.

(9) Jetti, R. K. R.; Boese, R.; Thallapally, P. K.; Desiraju, G. R. *Cryst. Growth Des.* **2003**, *3*, 1033.

(10) Vishweshwar, P.; Nangia, A.; Lynch, V. M. *J. Org. Chem.* **2002**, *67*, 556.

(11) Zyss, J.; Ledoux-Rak, I.; Weiss, H.-C.; Bläser, D.; Boese, R.; Thallapally, P. K.; Thalladi, V. R.; Desiraju, G. R. *Chem. Mater.* **2003**, *15*, 3063.

(12) Desiraju, G. R. *Acc. Chem. Res.* **2002**, *35*, 565.

(13) Scheiner, S.; Kar, T.; Pattanayak, J. *J. Am. Chem. Soc.* **2002**, *124*, 13257.

(14) Sarkhel, S.; Desiraju, G. R. *Proteins* **2004**, *54*, 247.

(15) Tarakeshwar, P.; Kim, K. S.; Brutschy, B. *J. Chem. Phys.* **1999**, *110*, 8501.

(16) Riehn, C.; Reimann, B.; Buchhold, K.; Vaupel, S.; Barth, H.-D.; Brutschy, B.; Tarakeshwar, P.; Kim, K. S. *J. Chem. Phys.* **2001**, *115*, 10045.

(17) Buchhold, K.; Reimann, B.; Djafari, S.; Barth, H.-D.; Brutschy, B.; Tarakeshwar, P.; Kim, K. S. *J. Chem. Phys.* **2000**, *112*, 1844.

(18) Riehn, C.; Buchhold, K.; Reimann, B.; Djafari, S.; Barth, H.-D.; Brutschy, B.; Tarakeshwar, P.; Kim, K. S. *J. Chem. Phys.* **2000**, *112*, 1170.

(19) Brutschy, B. *Chem. Rev.* **2000**, *100*, 3891.

(20) Venkatesan, V.; Fujii, A.; Ebata, T.; Mikami, N. *Chem. Phys. Lett.* **2004**, *394*, 45.

(21) Ebata, T.; Fujii, A.; Mikami, N. *Int. Rev. Phys. Chem.* **1998**, *17*, 331.

(22) Frisch, M. J.; Trucks, G. W.; Schlegel, H. B.; Scuseria, G. E.; Robb, J. M. A.; Cheeseman, R.; Zakrzewski, V. G.; Montgomery, J. A., Jr.; Stratmann, R. E.; Burant, J. C.; Dapprich, S.; Millam, J. M.; Daniels, A. D.; Kudin, K. N.; Strain, M. C.; Farkas, O.; Tomasi, J.; Barone, V.; Cossi, M.; Cammi, R.; Mennucci, B.; Pomelli, C.; Adamo, C.; Clifford, S.; Ochterski, J.; Petersson, G. A.; Ayala, P. Y.; Cui, Q.; Morokuma, K.; Malick, D. K.; Rabuck, A. D.; Raghavachari, K.; Foresman, J. B.; Cioslowski, J.; Ortiz, J. V.; Baboul, A. G.; Stefanov, B. B.; Liu, G.; Liashenko, A.; Piskorz, P.; Komaromi, I.; Gomperts, R.; Martin, R. L.; Fox, D. J.; Keith, T.; Al-Laham, M. A.; Peng, C. Y.; Nanayakkara, A.; Gonzalez, C.; Challacombe, M.; Gill, P. M. W.; Johnson, B.; Chen, W.; Wong, M. W.; Andres, J. L.; Gonzalez, C.; Head-Gordon, M.; Replogle, E. S.; Pople, J. A. *Gaussian 98*, revision A.7; Gaussian, Inc.: Pittsburgh, PA, 1998.

(23) Kim, K. S.; Tarakeshwar, P.; Lee, J. Y. *Chem. Rev.* **2000**, *100*, 4145.

(24) Boys, S. F.; Bernardi, F. *Mol. Phys.* **1970**, *19*, 553.

(25) Okuyama, K.; Kakinuma, T.; Fujii, M.; Mikami, N.; Ito, M. *J. Phys. Chem.* **1986**, *90*, 3948.

(26) Shimanouchi, T. *Tables of Molecular Vibrational Frequencies*; National Standard Reference Data Series; USGPO: Washington, DC, 1972; Vol. I.

(27) Bingnall, O. N.; Hunt, R. H.; Shelton, W. N. *J. Mol. Spectrosc.* **1994**, *166*, 137.

(28) Hunt, R. H.; Shelton, W. N.; Cook, W. B.; Bignall, O. N.; Mirick, J. W. *J. Mol. Spectrosc.* **1991**, *149*, 252.

(29) Kalasinsky, V. F.; Anjaria, H. V. *J. Phys. Chem.* **1980**, *84*, 1940.

(30) Senent, M. L.; Perez-Ortega, A.; Arroyo, A.; Domínguez-Gómez, R. *Chem. Phys.* **2001**, *266*, 19.

(31) Senent, M. L.; Niño, A.; Muñoz-Caro, C.; Smeyers, Y. G.; Domínguez-Gómez, R.; Orza, J. M. *J. Phys. Chem. A* **2002**, *106*, 10673.

(32) Alkorta, I.; Rozas, I.; Jimeno, M. L.; Elguero, J. *Struct. Chem.* **2001**, *12*, 459.

(33) Hunter, E. P.; Lias, S. G. *J. Phys. Chem. Ref. Data* **1998**, *27*, 413.